

A 640 kyr geomagnetic and palaeoclimatic record from Lake Baikal sediments

Vadim A. Kravchinsky,¹ Michael E. Evans,¹ John A. Peck,² Hideo Sakai,³
Mikhail A. Krainov,⁴ John W. King⁵ and Mikhail I. Kuzmin⁴

¹Institute for Geophysical Research, Physics Department, University of Alberta, Edmonton, AB, Canada T6G 2J1. E-mail: vkrav@phys.ualberta.ca

²Department of Geology, University of Akron, Akron, OH 44325-4101, USA

³Department of Earth Sciences, Faculty of Science, Toyama University, Gofuku 3190, Toyama 930, Japan

⁴Institute of Geochemistry, Siberian Branch of Russian Academy of Science, 664033 Irkutsk, Russia

⁵Graduate School of Oceanography, University of Rhode Island, Narragansett, RI 02882-1197, USA

Accepted 2007 February 17. Received 2007 February 16; in original form 2005 May 9

SUMMARY

Magnetic remanence vectors for 1737 samples from two ~100 m cores of Lake Baikal sediments are reported along with complete magnetic susceptibility profiles obtained from a pass-through system. Chronological control is established by means of two independent correlations; first, by matching susceptibility variations to the oceanic oxygen isotope record and second, by matching the relative palaeointensity variations to the SINT-800 global reference curve. These both imply an average deposition rate of 15 cm kyr⁻¹ and a basal age of ~640 ka. Spectral analysis reveals the presence of Milankovitch signals at ~100 kyr (eccentricity), ~41 kyr (obliquity) and ~23 and ~19 kyr (precession). Stable remanence vectors are almost all of normal polarity. The few exceptions comprise brief intervals of low and/or negative inclinations which probably represent geomagnetic excursions. However, these are far less numerous than the high sedimentation rate would lead one to expect. Furthermore, only four of them can be readily matched to the—still poorly understood—global pattern. These are the Laschamp, the Albuquerque, the Iceland Basin and perhaps the West Eifel excursions which occurred at ~38 000, ~146 000, at 180 000–190 000 and at 480 000–495 000 yr ago, respectively.

Key words: geomagnetic excursions, Lake Baikal, magnetic susceptibility, Milankovitch cycles, palaeoclimate, Siberia

INTRODUCTION

Lake Baikal is the largest (23 000 km³), deepest (>1600 m) and oldest (~20 × 10⁶ yr) lake on Earth. It is located in southeastern Siberia in a continental rift zone that ultimately owes its origin to the indentation tectonics resulting from the collision of India and Asia (Tapponier *et al.* 1982). Palaeomagnetic investigations of sediments in and around the lake have been carried out since the 1980s (Kravchinsky and Mats 1982; King *et al.* 1993; Peck *et al.* 1994, 1996). These studies indicated that the sediments involved are suitable for palaeomagnetic and palaeoclimatic investigations, both in terms of their basic magnetic properties and in terms of the chronological control available. This latter point is particularly well illustrated by drilling results from the Academician Ridge, a topographic high separating the central and northern basins of the lake, where water depths of less than 300 m are common. For the last 5 Myr, sediments there accumulated continuously at a rate of about 4 cm kyr⁻¹ (Williams *et al.* 1997; Kravchinsky *et al.* 1998). Recently, the existence of this steady depositional regime has been extended back to 6.7 Myr (Kravchinsky *et al.* 2003).

Most long palaeoclimatic archives, spanning several million years, have been obtained from oceanic sediment cores (Imbrie *et al.* 1984) or from thick continental sequences of loess (Heller and Evans 1995). Lake deposits generally represent much shorter time intervals, typically on the order of tens of thousands, occasionally a few hundred thousand years. In terms of their time span, the Lake Baikal sediments offer the unique possibility of obtaining very long, continuous profiles of past global change and significant progress on this task has already been made (Williams *et al.* 1997; Kravchinsky *et al.* 2003). In this paper, however, we report detailed results from the Buguldeika Saddle situated some 200 km southwest of the Academician Ridge, opposite the delta of the Selenga River (Fig. 1). Here, the sedimentation rate is much higher than on the Academician Ridge, so that the ~100 m cores obtained are entirely restricted to the Brunhes Chron. The central objective, therefore, was to pursue the possibility of higher resolution comparisons with other palaeoclimate proxies, notably the oceanic oxygen isotope record. It was also hoped that the magnetic remanence data would reveal the presence of some, or all, of the many polarity subchrons and/or geomagnetic excursions that have been variously reported

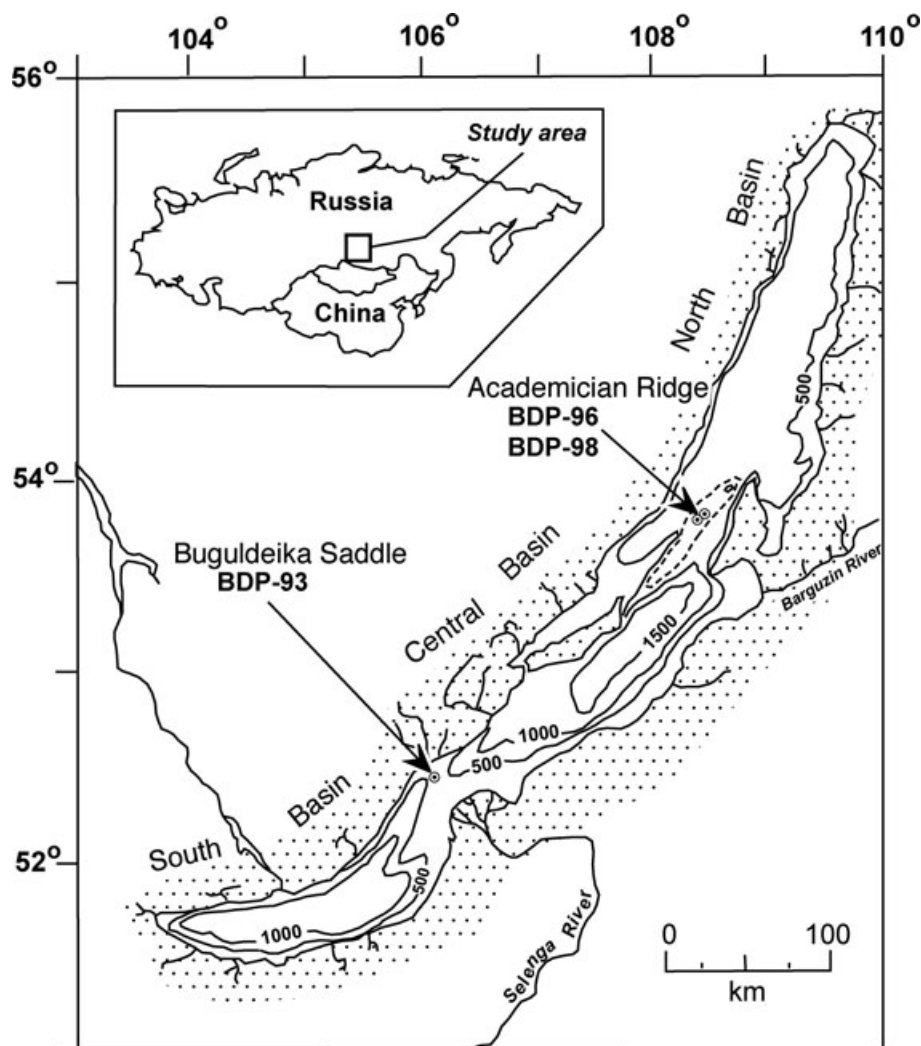


Figure 1. Simplified map of Lake Baikal showing the 1993, 1996 and 1998 drill sites.

within the Brunhes and about which considerable uncertainty still exists.

GEOLOGICAL SETTING

The Buguldeika drilling site is situated at $106^{\circ}09'11''\text{E}$, $52^{\circ}31'05''\text{N}$ between the central and southern basins of Lake Baikal and close to the mouth of the Buguldeika River (Fig. 1). Hydraulic piston cores (57 mm-diameter) were taken from two holes that were only a few metres apart, BDP-93-1 (98 m, 72 per cent recovery) and BDP-93-2 (102 m, 90 per cent recovery) (BDP-93 members 1995). The course of the Buguldeika River traverses a variety of geological structures and lithologies. Granite, gneiss and metamorphic rocks of amphibolite and granulite facies are widespread. The Primorsky Range, where the river has its source, is characterized by Riphean phosphorites and Cambrian carbonates. The drainage basin as a whole has a widespread laterite-kaolinite weathering crust of Cretaceous-Palaeogene age. Mats (1993) gives a thorough description of the geology of the whole region.

Seismic data in this area of Lake Baikal define a reflector that corresponds to a marked lithological change observed in the cores (BDP-93 members 1995). Above ~ 58 m the sediments are fine grained and consist of a rhythmic alternation of two lithologies, one

composed of a mixture of silt and clay containing up to 30 per cent diatom opal, the other composed mostly of clay containing less than 3 per cent diatom opal. The depositional regime was interpreted as one in which periodic input of material by suspension flows, wind transport and ice-rafting is superimposed on a steady background of pelagic sedimentation from the water column. Below 58 m the sediments are often coarser grained with abundant turbidites in pelitic material that includes interbedded sand and silt. Biogenic silica data was acquired in detail for the uppermost 50 m of the core BDP-93-2 (Colman *et al.* 1999) but below 50 m published data on biosilica are not available. For hole BDP-93-1 (BDP-93 members 1997) the biosilica data have a resolution too low to be useful for our analysis.

METHODS

Low-field ($8 \mu\text{T}$), low-frequency (0.565 kHz), whole-core magnetic susceptibility (k) for both holes was measured at 3 cm intervals with a Bartington Instruments susceptibility meter. The pass-through loop sensor allowed entire core segments to be measured rapidly and non-destructively. The loop diameter was 72 mm and spatial resolution was 20–30 mm. Samples were taken in 5 cm³ plastic boxes at 30 cm intervals from core BDP-93-1 and at 2 cm intervals from BDP-93-2. They were distributed among the various laboratories

in the countries involved in this international project (Russia, USA, Japan and Canada) and measured independently. Preliminary results have already been published (BDP-93 members 1995, 1997; Sakai *et al.* 2001). Interlaboratory comparisons were performed in two ways, (1) a set of 48 samples was measured (NRM and magnetic susceptibility) in each laboratory and (2) more than 200 stratigraphically neighbouring samples (spanning the entire depths of the cores) were AF demagnetized in each laboratory. No important differences were observed.

The natural remanent magnetization (NRM) of the plastic-box samples was measured on a three-axis SCT cryogenic magnetometer at the University of Rhode Island, on a Molspin magnetometer at the University of Alberta, on a LAM-24 astatic magnetometer and a JR-4 rock-generator at the Irkutsk Palaeomagnetic Laboratory, and on a 2-G cryogenic magnetometer at the University of Toyama. Pilot samples representing all lithological types were taken from different depths spanning both cores (40 samples from hole 1, 68 from hole 2), especially in the intervals where excursions were expected. These were step-wise demagnetized in alternating fields (AF) up to 100 mT in order to find a suitable blanket treatment for the rest of the samples. On the basis of the results obtained it was decided to demagnetize the remaining samples at 10 mT, with numerous checks at 5, 20, 40 and 100 mT. The entire study involved a total of 1737 samples, 223 from BDP-93-1 and 1514 from BDP-93-2.

In addition to the analysis of the natural remanence of the samples, anhysteretic (ARM) and isothermal (IRM) remanences for representative samples from hole 1 were also determined for mineral magnetic purposes and for estimating relative palaeointensities. ARM was given in a Schonstedt GSD-1 demagnetizer operating at a peak AF field of 0.1 T with a steady bias field of 0.1 mT. IRM was given in a field of 1.2 T.

AGE MODEL

A critical requirement for our purposes is an adequate age model that allows depth to be converted into geological time. To derive such a timescale, we use two independent approaches, the first in-

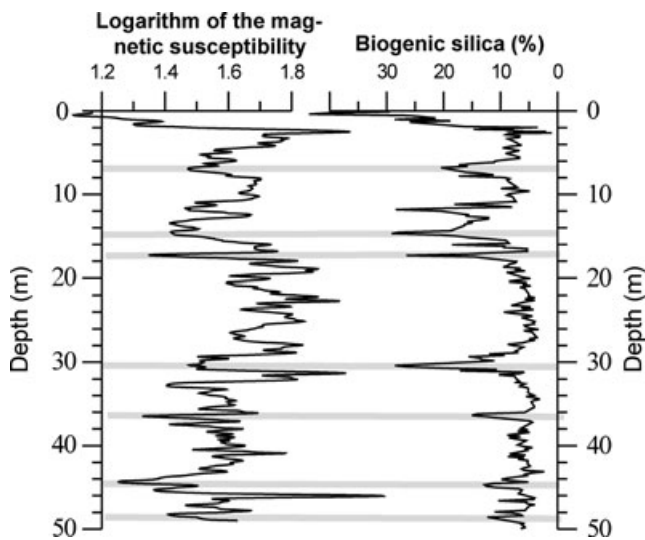


Figure 2. Correlation between whole-core magnetic susceptibility and biogenic silica profiles from hole BDP-93-2 (the only one for which high-resolution silica measurements were made). Logarithm of susceptibility in 10^5 SI units (after 15-point smoothing) is plotted. Biogenic silica data are taken from Colman *et al.* (1999) and given in wt% (note reversed scale).

Table 1. Tie points obtained from correlation of whole-core magnetic susceptibility of BDP-93-1 and BDP-93-2 and δO^{18} curve of the MD900963 (Bassinot *et al.* 1994). Bold numbers indicate the tie lines that are illustrated in Fig. 4.

BDP-93-1		BDP-93-2	
Depth (m)	Age (ka)	Depth (m)	Age (ka)
0	0	0	0
2.79	16	2.55	16
6.76	52	7.02	52
9.9	68	10.68	68
10.77	78	11.61	78
12.11	88	12.60	88
12.85	96	13.56	96
15.18	106	16.00	106
16.55	122	17.29	122
–	–	18.04	134
–	–	22.25	158
–	–	24.38	170
–	–	25.06	174
26.72	192	26.41	192
–	–	27.97	202
–	–	31.37	224
31.81	234	32.62	234
–	–	33.40	248
43.88	288	–	–
–	–	40.90	296
49.56	328	44.21	328
49.86	342	46.07	342
–	–	47.85	358
–	–	49.57	374
56.52	408	54.33	408
–	–	63.11	454
70.77	478	69.04	478
–	–	73.09	500
77.29	524	76.03	524
–	–	78.69	532
90.11	574	84.81	574
–	–	92.50	614
100.14	630	93.51	630

volving comparisons of magnetic susceptibility (MS) and biosilica data to the oceanic oxygen isotope record, the second comparing the relative palaeointensity record to the SINT-800 global summary.

As shown in several earlier Lake Baikal studies, magnetic susceptibility has a strong inverse correlation with biogenic silica variations (King *et al.* 1993; Peck *et al.* 1994, 1996; Kravchinsky *et al.* 2003). Diatomaceous organisms that produce biogenic silica are more productive during warmer climatic conditions and the concentration of biogenic silica is thus higher in interglacial intervals than in the intervening colder glacial intervals. Because silica is diamagnetic it decreases the observed susceptibility values during relatively warm intervals and leads to the climate signal visible in Fig. 2. A correlation is, therefore, expected between Lake Baikal magnetic susceptibility and oceanic oxygen isotope records. The BDP-96 and BDP-98 magnetic and biosilica data (Williams *et al.* 1997; Kravchinsky *et al.* 1998, 2003) and the ODP-677 (Shackleton *et al.* 1990) and MD900963 δO^{18} curves (Bassinot *et al.* 1994) indicate that this is indeed the case. The MS signal appears to be more detailed than the biogenic silica record because the dilution by biogenic silica is not the only factor able to affect the MS signal. Peck *et al.* (1994) demonstrated that relatively cold intervals in the Lake Baikal sediments are characterized by higher concentrations

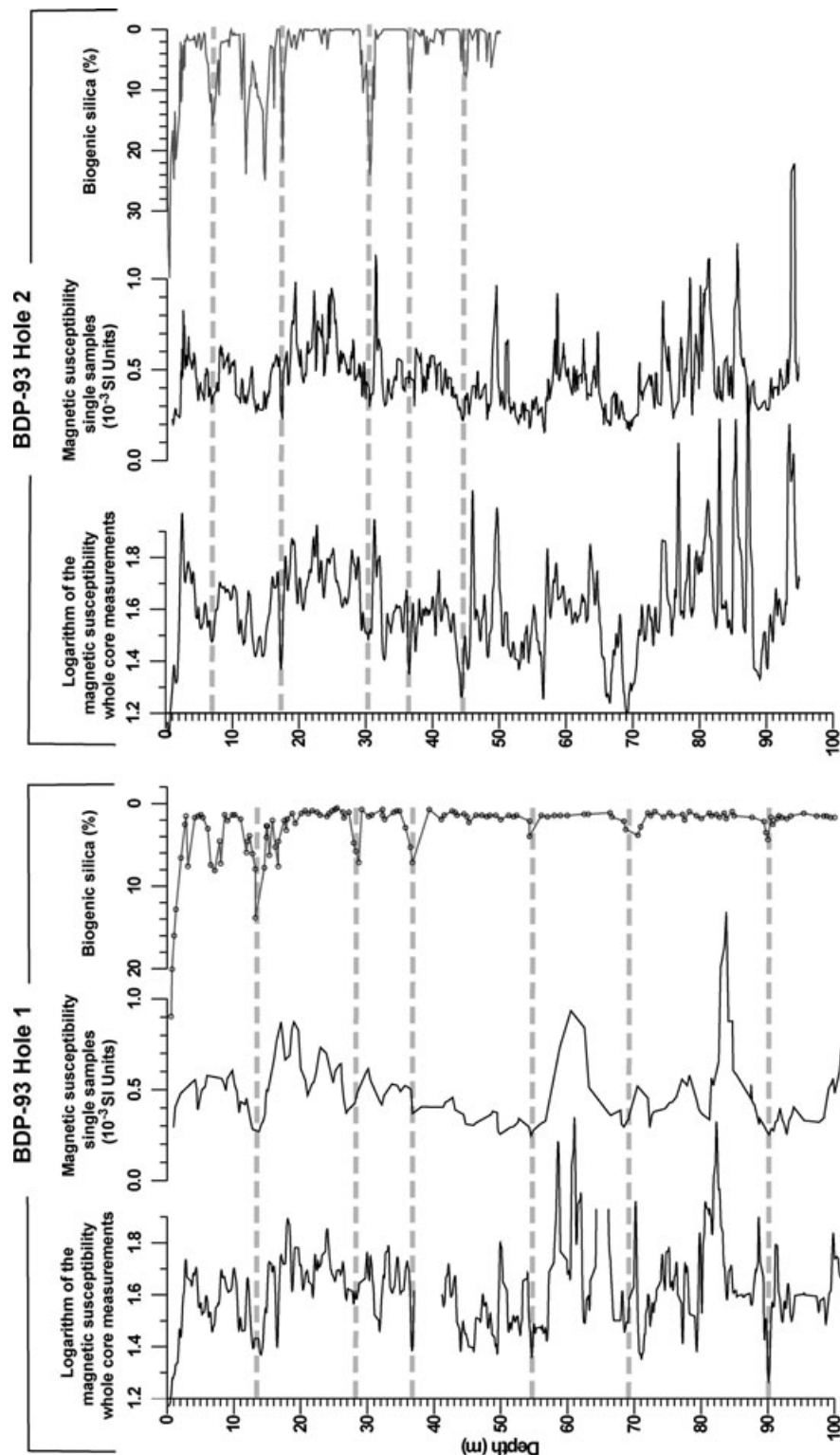


Figure 3. Correlation between whole-core magnetic susceptibility, single sample susceptibility and biogenic silica profiles from holes BDP-93-1 and BDP-93-2. Logarithm of whole-core susceptibility (after 15-point smoothing) is plotted. Biogenic silica data are taken from BDP-93 members (1995) for hole 1 and Colman *et al.* (1999) for hole 2 and given in wt% (note reversed scale).

of clay and magnetic minerals, high coercivity minerals and larger magnetic grain size, higher density and sedimentation rates and lower biogenic silica accumulation. Although magnetic susceptibility mirrors the biogenic silica content for the main features (when both profiles have high resolution), details of the profiles are still

slightly better pronounced in the susceptibility record. Biogenic silica content does not always correlate perfectly in terms of amplitude of the signal with every short cold/warm interval, probably because of complexities arising from evolution, extinction and developing of different species.

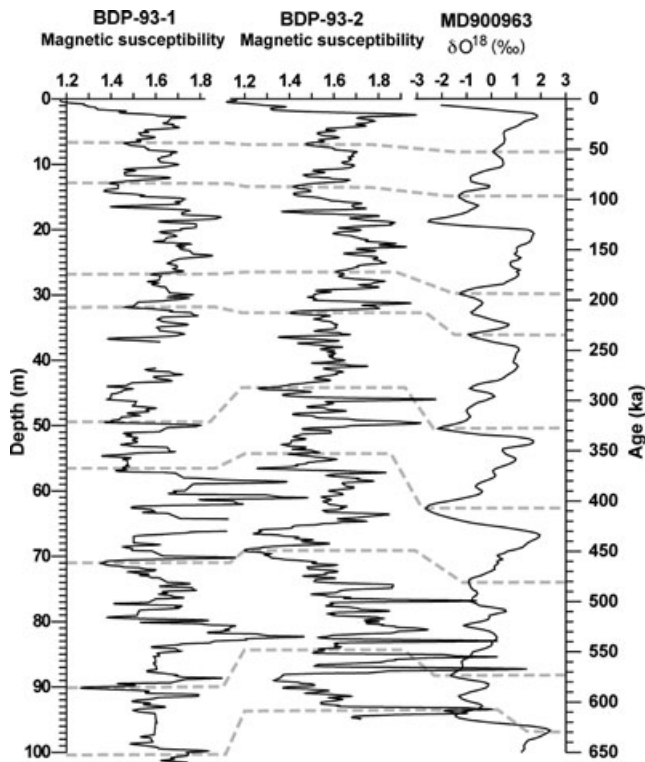


Figure 4. Correlation between whole-core magnetic susceptibility profiles (BDP-93-1 and BDP-93-2) (after 15-point smoothing, logarithm of the susceptibility) and δO^{18} oxygen isotope curve from MD900963 (Bassiot *et al.* 1994), which, in turn, reflects variations in global ice volume.

In Fig. 3, MS for the whole core and for plastic-box samples are compared to each other and to the biogenic silica record. Dashed horizontal lines demonstrate correspondence of major peaks for all three curves. Single sample MS and biogenic silica measurements for hole 1 have low resolution (sampling every ~ 30 – 50 cm, sometimes more) compared to whole core susceptibility measurements (every 2 cm). This explains why we could correlate only the main features of hole 1 where finer details are missed. Correlation between whole core and single sample susceptibility along with biogenic silica for the second hole is much more straightforward because the resolution of all the parameters is high. All major peaks of both susceptibility records can be clearly seen and correlated with the most significant peaks in the biogenic silica record. It can also be seen that magnetic susceptibility has much higher resolution than biogenic silica.

In Fig. 4, we compare the susceptibility profiles of both BDP-93 cores to the proxy for the global ice volume record (MD900963) for the last 640 kyr. Agreement between hole 1 and hole 2 susceptibility profiles is good, and correlation of the more prominent maxima and minima to the δO^{18} curve is relatively straightforward. It leads to the tie points listed in Table 1, some of which are also indicated in Fig. 4 to guide the eye. In view of the close similarity between the susceptibility curves for the two cores we have combined them into a single profile, plotted as a function of time (Fig. 5). This allows the 4 m gap near 40 m in hole 1, and others too small to represent in Figs 3 and 4, to be covered by the data from hole 2. Magnetic susceptibilities of the individual cores 1 and 2 are plotted on a common age scale to demonstrate the fit between all the major features. Most of the peaks fit each other perfectly, others have different amplitudes or are slightly shifted, which can be explained by minor imperfections

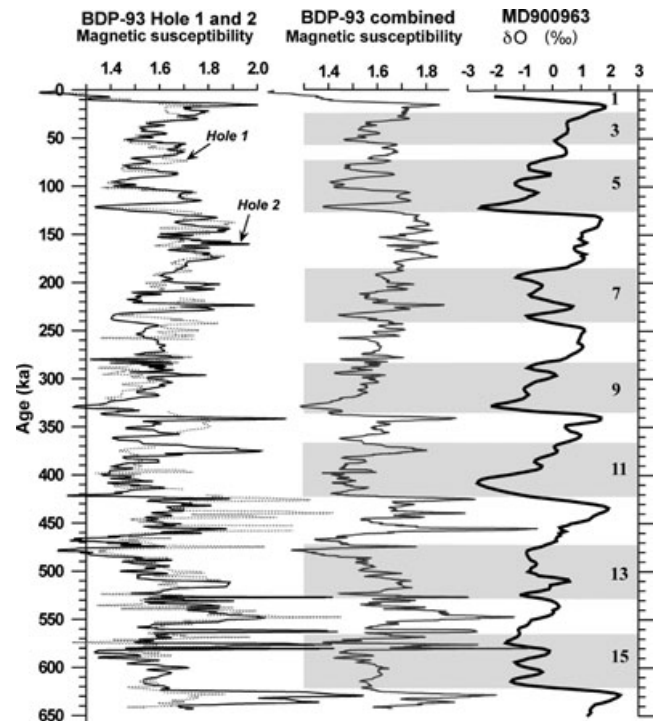


Figure 5. Magnetic susceptibility profiles for the BDP-93-1 (dashed line) and the BDP-93-2 (solid line) versus time and combined magnetic susceptibility profile from both records versus time. For convenience, the δO^{18} curve from MD900963 is included and the oxygen isotope stages (numbered) are indicated by shading. The combined susceptibility profile is smoothed slightly more (21-points) than the individual curves of Fig. 4 because of the increased number of data points.

in the age model. The correlation was verified further with relative palaeointensity and biogenic silica data sets (see below). The cores were combined by putting their susceptibility data on a common age scale by linear interpolation between the tie points of Table 1 and averaging the two values whenever their ages were identical. The resulting curve was smoothed by a least-squares method and then resampled at 1 kyr interval. It appears that, even after smoothing, this interior continental site is more sensitive to high-frequency climatic fluctuations than is the marine record.

Fig. 6 demonstrates the correspondence between the biogenic silica of BDP-93 hole 2 (Colman *et al.* 1999) and the previously published BDP-96 hole 2 (Williams *et al.* 1997; Prokopenko *et al.* 2001). It also shows the correlation between the silica data, our combined MS profile and the MD90093 oxygen isotope curve (Bassiot *et al.* 1994). The correlation is straightforward. For example, isotope stage 5 has three major peaks that can be seen in all four records. Although the three large peaks in stage 7 can be correlated in three of the profiles (biosilica 96, MS 93 and oxygen isotope), only one peak is represented in the biogenic silica BDP-93 record. This demonstrates that MS is preferable for constructing the BDP-93 age model.

BDP-93 members (1997) showed that inferred interglacial periods are characterized by low magnetic concentrations (k , k_{ARM} , SIRM) and a composition dominated by low coercivity minerals (HIRM, S-ratio). Inferred glacial periods are characterized by higher magnetic concentrations and increased amounts of high coercivity minerals (see fig. 10 in BDP-93 members 1997). During warm periods increased diatomaceous sedimentation, resulting from increased lake productivity, diluted the magnetic concentration. At the same

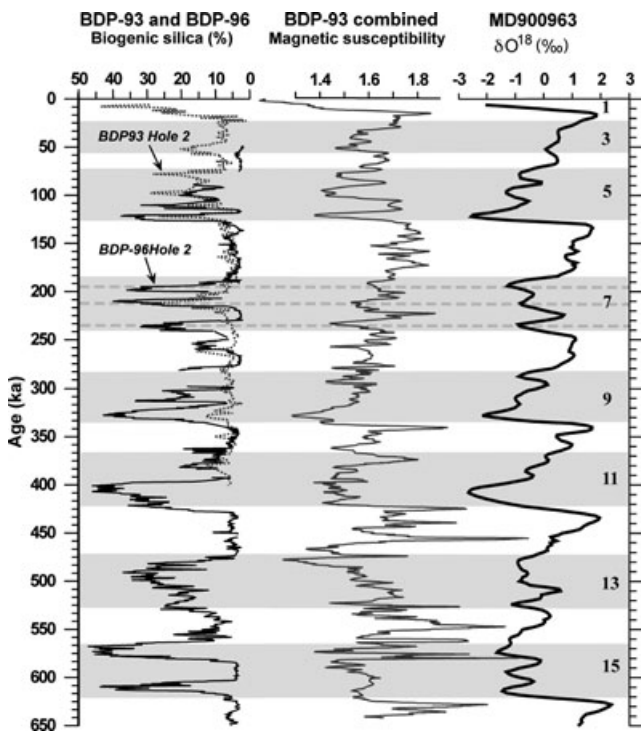


Figure 6. Comparison of the biogenic silica record for BDP-93-2 (dashed line) and BDP-96-2 (solid line) holes. Major peaks correlate although BDP-93-2 has lower resolution. Combined magnetic susceptibility profile from both records versus time and the δO^{18} curve from MD900963 is included for visual correlation of the major warm/cold events. The oxygen isotope stages are indicated by shading and are numbered. Horizontal dashed lines indicate correspondence of three major warming events for all records in oxygen isotope stage 7.

time enhanced soil development in the Selenga and Buguldeika River catchments yielded increased amounts of low coercivity minerals. Below 50 m the magnetic concentration generally increases, low coercivity minerals dominate and increased amounts of sand and gravel are present. These magnetic and lithological changes suggest a change in deposition environment and rate of sedimentation that could mask the biogenic silica signal. However, some layers with higher biosilica are still observed (BDP-93 members 1997).

Peck *et al.* (1996) studied seven 2–9 m gravity cores in the Buguldeika area and concluded that the normalized palaeointensity records meet all the criteria of King *et al.* (1983) and Tauxe (1993) concerning homogeneity, composition, concentration and size of magnetic carriers. We therefore carried out the appropriate measurements on plastic-box samples in an attempt to construct a relative palaeointensity record spanning ~100 m. Fig. 7 illustrates the downcore variations in magnetic parameters that are often used for this purpose. The magnetic susceptibility curve compares favourably with the pass-through data (see Fig. 3), but with lower resolution; the main maxima at depths of 3, 8, 18, 60 and 82 m can be easily observed. From Fig. 7 it can be seen that magnetic susceptibility and NRM after AF demagnetization at 10 mT have generally coherent variations suggesting that the NRM also contains variations that are driven by environmental changes. This probably reflects variations in the concentration of magnetite, which are also seen in the ARM profile. Two short intervals near 58 and 83 m were not used for further analysis of relative palaeointensity as they consist of coarse sandy layers and gravel with anomalously high magnetic signals. Apart from these two exceptions, the variations

of k , NRM and ARM do not exceed an order of magnitude, as required for sedimentary palaeointensity records (Tauxe 1993). The ratio k_{ARM}/IRM is usually regarded as an indicator of magnetic grain size (Thompson and Oldfield 1986; Maher 1988; Yu and Oldfield 1989; Bloemendal *et al.* 1993). In our case this ratio ranges from 10×10^{-5} to 40×10^{-5} , typical of single domain to pseudo-single domain magnetite, again satisfying the requirements for relative palaeointensity estimations (Tauxe 1993).

Fig. 8 illustrates the NRM_{10mT}/ARM profile for hole 1 and the NRM_{10mT}/k profiles for both holes 1 and 2. The choice of normalization parameter is still a matter of debate, although a comparison between different procedures shows that 'any technique can be used with confidence, provided that the characteristic component has been properly isolated and the sediments are magnetically homogeneous' (Valet and Meynadier 1998). The BDP-93 profiles are compared to the SINT-800 global reference intensity curve of Guyodo and Valet (1999) and the tie points obtained are listed in Table 2. Our palaeointensity record, although less detailed, correlates well with known records from Lake Baikal in terms of the main features (Peck *et al.* 1996; Demory *et al.* 2005; Oda 2005).

However, a difficulty arises with the rapid change seen at ~15 m (see Fig. 8) because a similar jump occurs in the mineral magnetic profiles (in particular, see k_{ARM}/IRM plot in Fig. 7). This raises the issue of lithological control of the observed relative palaeointensities. For the cores as a whole there is no obvious control; the correlation coefficients between palaeointensity and susceptibility profiles are very small ($R = 0.26$ and 0.062 for holes 1 and 2, respectively). Post-depositional dissolution of small magnetite particles is a possibility although, where it has been identified, this mechanism is restricted to the top metre or less (Peck and King 1996; Dearing *et al.* 1998).

Fig. 9 summarizes all the evidence that provides chronological control. In addition to the susceptibility, biogenic silica and relative palaeointensity evidence discussed above, we also note that the uppermost 2.5 m was dated by the radiocarbon method (Colman *et al.* 1999) which indicates that the age of the surface sediments is zero (i.e. sedimentation is continuing today). Seismic and lithologic data do not show evidence for any major discontinuities, so the sedimentation is considered to be—broadly speaking—continuous (BDP-93 members 1997). Also, a uranium-series isochron age of 185 ± 9 kyr was obtained by Sandimirov and Pampura (1995) on bulk sediment from 26 to 30 m depth interval of core BDP-93-1. The resulting plots provide a coherent picture implying average sedimentation rates of ~14 and ~19 $cm kyr^{-1}$ above and below the seismic reflector at ~58 m, respectively. Fig. 10 demonstrates that the sedimentation rates obtained by correlation of different parameters do not vary too greatly. Better core recovery and denser sampling for hole 2 leads to better agreement between sedimentation rates obtained by different methods (Fig. 10B). This is in agreement with the lithological evidence which demonstrates that sediments below 50 m are coarser than sediments above (BDP-93 members 1997; Horii *et al.* 2001). BDP-93 members (1997) also showed that biogenic silica, although still present, is relatively diluted in the lower part of the core. This independently demonstrates that rates of sedimentation should be higher in the lower part of the cores and agrees with our age model.

Following the recommendation of Tauxe (1993), we decided to investigate the coherence between k and palaeointensity estimates. For hole 2, we did this for the entire core and also for the parts above and below 15 m, separately. This was done because of the marked change in amplitude at 15 m depth (see Fig. 8). Coherence values for the whole cores NRM_{10mT}/k versus k (hole 2) and NRM_{10mT}/ARM versus ARM (hole 1) were calculated. Fig. 11A

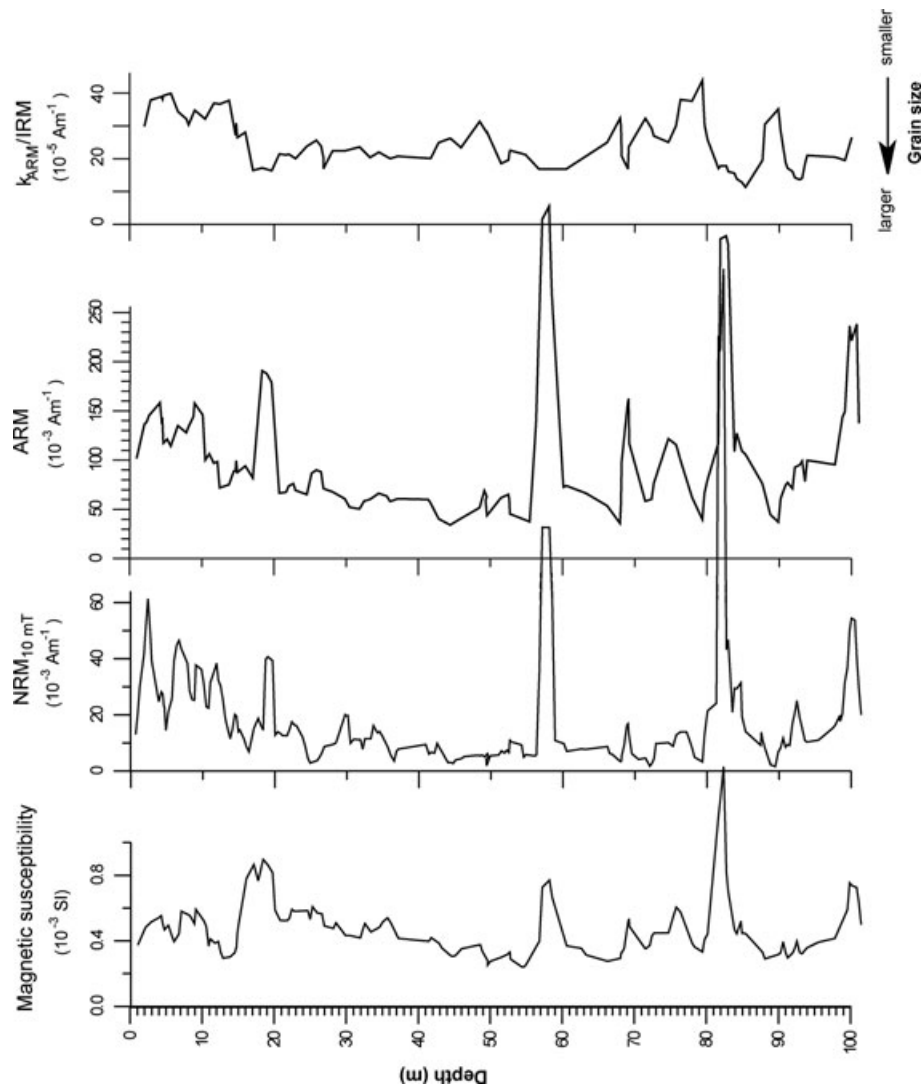


Figure 7. Downcore variations of certain magnetic parameters for plastic-box samples from hole BDP-93-1; magnetic susceptibility (plotted on a logarithmic scale), natural remanent magnetization after 10 mT AF treatment, ARM and ARM susceptibility/IRM. See text for experimental details.

demonstrates that single sample magnetic susceptibility, which was used as a palaeointensity normalizer, has power at the eccentricity and precession astronomical periodicities and, therefore, depends on lithological/palaeoclimatic changes. Relative palaeointensity (NRM/k) itself does not show any visibly similar periods. Squared coherence for the whole core is lower than 95 per cent confidence level which illustrates that the normalizer (k) is appropriate and the relative palaeointensity does not correlate with the normalizer itself (Fig. 11B). However when we calculated squared coherence for only the upper 15 m, we found that it exceeds the confidence limit at astronomical (Milankovitch) periods of 100, 41 and 23 kyr (Fig. 11C). This means that the relative palaeointensity record for the upper 15 m strongly depends on lithology and cannot be used further. The palaeointensity record below 15 m has some intervals where palaeointensity and its normalizer are coherent (Fig. 11D) but not at Milankovitch periods, so the palaeointensity record can be used to check our age model independently from biogenic silica and magnetic susceptibility records.

Coherence values for the NRM_{10mT}/ARM versus ARM (hole 1) are illustrated for the entire core (Fig. 11E) and for the upper 15 m (Fig. 11F). Fig. 11E does not demonstrate any significant coherence,

whereas the upper 15 m (Fig. 11F) shows significant coherence at very low non-Milankovitch frequencies. Overall, we may conclude that palaeointensity is a reliable record for both holes but results for the upper 15 m should be regarded with extreme caution.

FREQUENCY ANALYSIS

We have performed a variety of spectral analyses on the stacked magnetic susceptibility and biogenic silica profiles. For these purposes the age model based on magnetic susceptibility correlation was used. Before calculating the power spectra, we applied a least-squares smoothing from which we extracted equally spaced data points at 1 kyr intervals. Power spectra were then calculated by the Blackman-Tukey method with a Bartlett window (Blackman and Tukey 1958). The entire procedure follows that described by Paillard *et al.* (1996) and uses their software.

Fig. 12A illustrates the power spectrum for the entire 640 kyr of magnetic susceptibility data for BDP-93. The BDP-93 spectra can be compared with the various power spectra for the same time interval in cores from the Academician Ridge about 200 km away

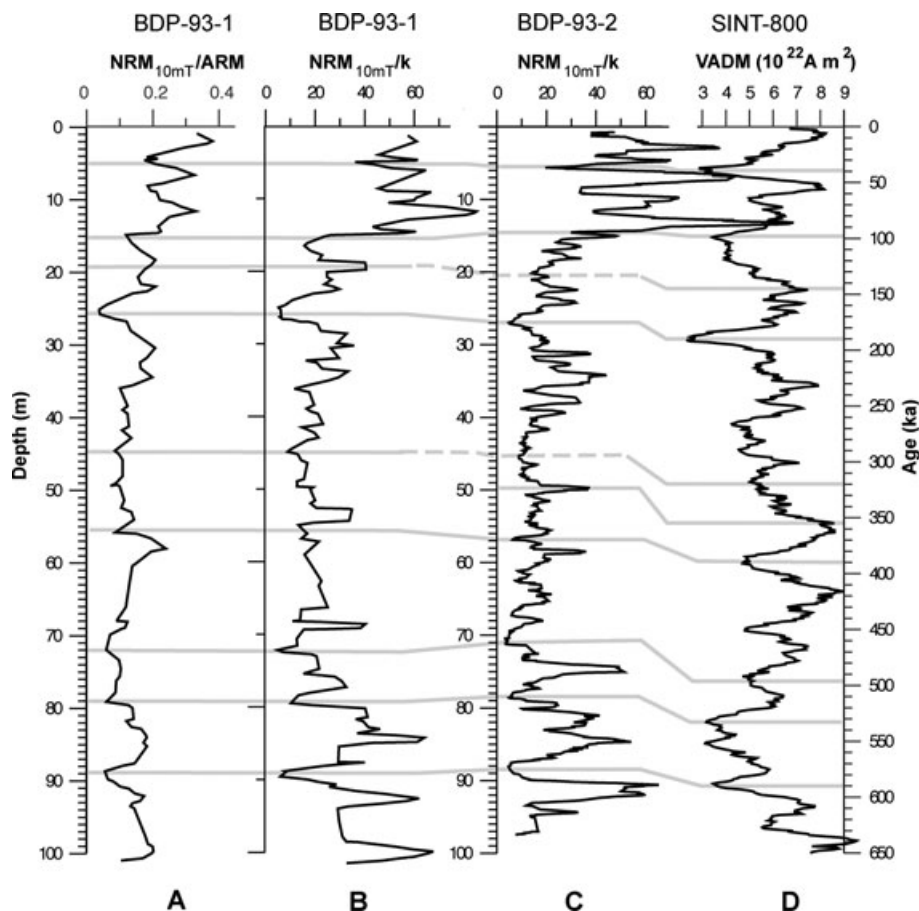


Figure 8. Comparison between the $\text{NRM}_{10\text{mT}}/\text{ARM}$ and $\text{NRM}_{10\text{mT}}/k$ profiles with the SINT-800 relative palaeointensity summary of Guyodo and Valet (1999).

(Kravchinsky *et al.* 2003) shown in Fig. 12B. In both figures, Milankovitch peaks at ~ 100 kyr (eccentricity) and ~ 41 kyr (obliquity) are clearly visible, as well as a non-Milankovitch peak at ~ 29 kyr. The Milankovitch precession peaks at ~ 19 and ~ 23 kyr are present in the BDP-93 data, but are muted or absent on the Academician Ridge. This may be due, at least in part, to the fact that the sedimentation rate on the Academician Ridge is much lower (~ 4 cm kyr $^{-1}$) than that found at the Buguldeika site (~ 14 cm kyr $^{-1}$ above 58 m, ~ 19 cm kyr $^{-1}$ below).

We then compared magnetic susceptibility and biogenic silica data for hole BDP-93-2, for which the biosilica data are limited to 400 kyr (Colman *et al.* 1999) (Fig. 12C). Because of lower time resolution of the available biogenic silica data the interpolation interval was increased to 2 kyr. The ~ 41 kyr obliquity and ~ 100 kyr eccentricity signals are clearly seen in both profiles, but the ~ 23 kyr precession signal is much more distinct in the biogenic silica record. Fig. 12D illustrates the strong coherence between these biosilica and susceptibility records in terms of Milankovitch cyclicity.

Regarding the 29 kyr power that appears consistently, it should be noted that Hinnov's (2000) analysis of Laskar's (1990) insolation calculations for the last 10 Myr yields peaks at 29 and 54 kyr in addition to the Milankovitch obliquity peak at 41 kyr. Von Döbenek and Schmieder (1999) also observed these peaks. Furthermore, Rial and Anaclerio (2000) show that the time-series of greenhouse gases and salt aerosols in the Vostok ice-core yield distinct spectral peaks at ~ 29 and ~ 69 kyr as well as other, smaller, peaks surrounding the ~ 40 kyr obliquity signal which they interpreted as sidebands

generated by frequency modulation of the obliquity signal itself. A similar peak at ~ 29 kyr was also found in magnetic and biogenic silica data of our previously published BDP-98 records (Kravchinsky *et al.* 2003). Mix *et al.* (1995) attribute this peak to non-linear interaction between the 41 and 100 kyr periods. Rial and Anaclerio (2000) point out that observations of non-linear responses of this kind are not often described in the literature. They consider that the main reason for this is that the tuning of most published records to the obliquity frequency destroys the effect of frequency modulation on the obliquity signal.

Finally, we note that the amplitude of the eccentricity signal is large in the susceptibility data of BDP-93 and in the biosilica data of BDP-96-2 and MS signal from BDP-96 and 98, as is the case in all ODP oxygen isotope records (Shackleton *et al.* 1990; Rial 1999; Hinnov 2000). However, the obliquity signal is still very strong in the BDP-96 and BDP-98 records.

GEOMAGNETIC EXCURSIONS

The results of AF demagnetization indicate that the sediments under investigation carry a strong and stable primary remanence, with median destructive fields (MDFs) between 20 and 30 mT. Typical demagnetization behaviour for pilot samples is shown in Fig. 13. The majority of the samples exhibit a single remanence component, but about 10 per cent of them give evidence of a present-field viscous overprint that could be removed by 10 mT AF demagnetization. The resulting inclination profiles are given in Fig. 14, which shows the

Table 2. Tie points obtained from correlation of the relative palaeointensity record to SINT-800 (Guyodo and Valet 1999). Bold numbers indicate the tie lines that are illustrated in Fig. 8.

BDP-93-1		BDP-93-2	
Depth (m)	Age (ka)	Depth (m)	Time (ka)
0	0	0	0
5.2	37	5.7	37
8.16	56	–	–
8.82	64	9.05	64
15.11	99	14.62	99
18.69	119	–	–
19.73	146	20.62	146
20.73	154	–	–
–	–	22.44	158
22.69	166	24.3	166
25.86	192	27.28	192
32.19	245	–	–
33.66	252	–	–
–	–	36.37	266
–	–	41.02	290
36.07	266	–	–
44.75	318	–	–
–	–	49.7	355
54.85	390	56.94	390
–	–	62.41	450
72.05	495	70.68	495
–	–	75.06	510
78.69	532	78.69	532
89.46	588	88.59	588
92.47	609	–	–
98.44	627	93.99	627

data for the two holes separately (plotted against depth) as well as the BDP-93-2 data plotted against time. The overall reliability of these profiles is attested by the data from 444 samples that were demagnetized to 20 mT. Of these, 428 moved less than 10° between the 10 and 20 mT demagnetization steps.

For most of their depth spans both cores indicate normal (i.e. Brunhes Chron) polarity (Fig. 14), as would be expected from the age model. However, there are several intervals of shallow or negative inclinations which may represent excursions of the geomagnetic field. Most of these consist of single isolated samples and cannot be regarded as firm evidence for genuine field behaviour. We

do not consider them further. There remain five shallow, or negative, inclination intervals in hole BDP-93-2 (at approximate depths of 5, 20, 27, 70 and 89 m), three of which are also present in BDP-93-1 (20, 26 and 69 m). Pilot samples in these intervals indicate that the directions observed are not due to unstable magnetization. After removal of a soft overprint, the remanence vectors decay linearly towards the origin indicating the presence of a stable primary component (Fig. 15). The two events that are recorded by multiple samples in both holes have the same ages according to their independently derived chronologies based on the two susceptibility profiles, which further supports our age model. Three of the shallow, or negative, inclination features found do not readily match any of the excursions that have been proposed by various authors (for summaries, see Opdyke and Channell 1996; Langereis *et al.* 1997; Oda 2005), but those near 5, 20, 27 and 70 m merit further discussion. They display convincing systematic directional patterns, shown expanded in Figs 16–19. Relative declinations were obtained by matching adjacent core segments at their ends. The excursion near 5 m (Fig. 16) with an age of ~ 37 –39 kyr fits perfectly with a minimum on our palaeointensity curve and in the SINT-800 pattern and can be identified as the Laschamp excursion. It can also be correlated with the single negative inclination point (-10°) at 4.55 m depth in core 1 (Fig. 14). Plenier *et al.* (2006) argue on the basis of new K-Ar and Ar-Ar dating that the Laschamp excursion is constrained within the interval 35.2–39.7 ka, which fits very well with our dating.

Another event near 20 m in hole 1 (only one sample) and 20.5 for the hole 2 (eight samples with negative inclinations mostly $\sim -60^\circ$) could represent the Albuquerque excursion (Fig. 17). The age of this excursion was suggested as 155–165 kyr by Langereis *et al.* (1997) but, in fact, it has a much wider range, possibly starting from ~ 140 kyr (140 ± 10 : Westgate *et al.* 1990; 141 ± 15 : Takai *et al.* 2002). Oda *et al.* (2005) determined the age of this excursion at 140–160 kyr. Following our age model we cannot correlate the Albuquerque excursion with any strong minimum in SINT-800, but there is a minor feature at ~ 150 ka that could potentially correspond to this excursion. Following our age model the excursion is relatively short and has an approximate age of 145–146 ka.

Near 27 m depth, relative declinations were reconstructed from three different core segments (15-1, 16-1 and 17-1) and also demonstrate excursions behaviour (Fig. 18). This excursion correlates very well with the relative palaeointensity minimum at ~ 26 m in BDP-93-1 and that at ~ 27 m in BDP-93-2 (Fig. 8). The main part

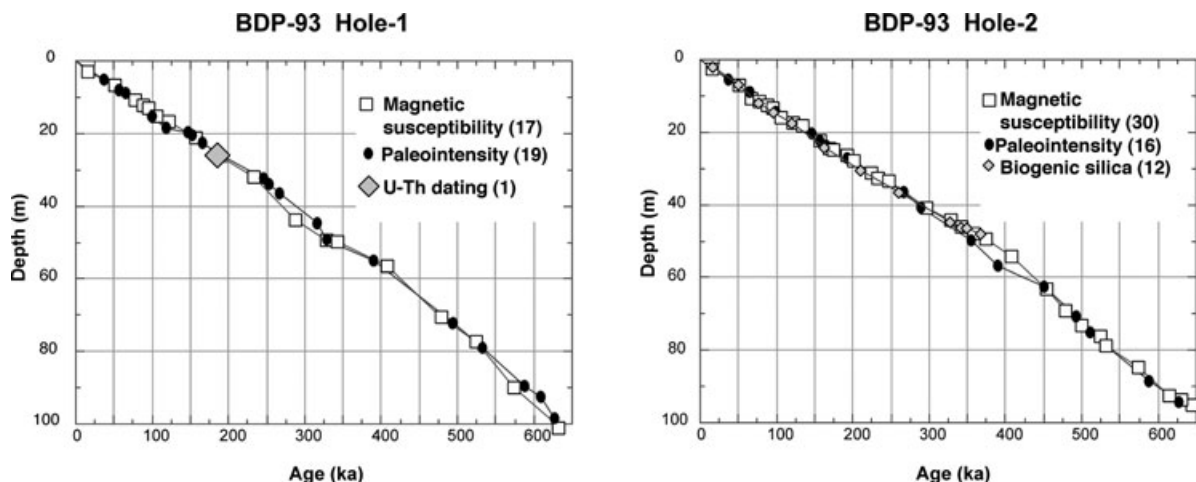


Figure 9. Age–depth relationships for holes 1 and 2 of BDP-93. The number of data points in each category is given in brackets.

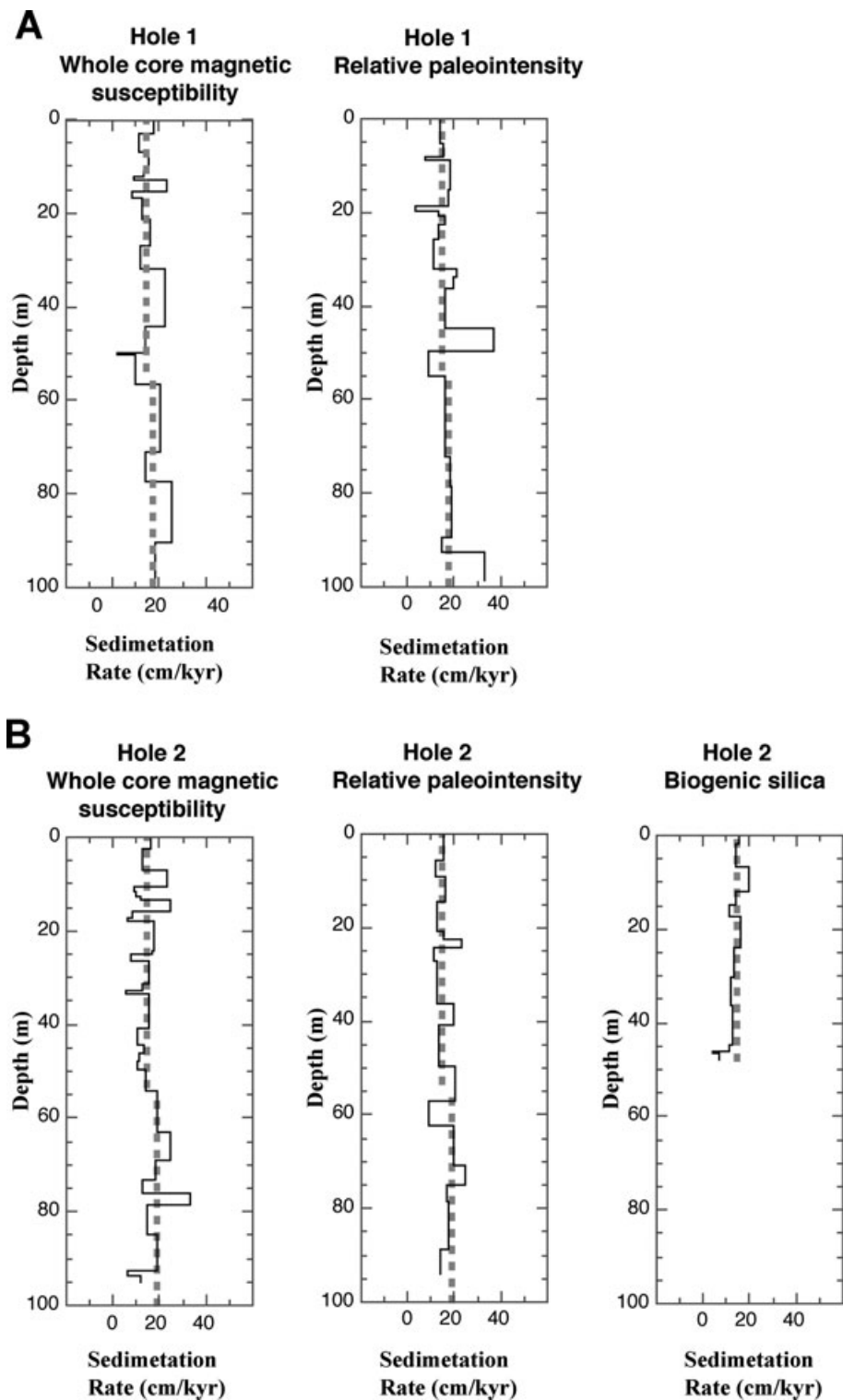


Figure 10. Sedimentation rates in cm kyr^{-1} obtained independently by different approaches. The dashed lines correspond to the slopes obtained from Fig. 9.

of this excursion appears to have lasted ~ 5000 yr, but the slow recovery to typical normal polarity inclinations (60° – 70°) may double this. Although the recovery seems to have been slow the onset of this excursion appears to have been very rapid, but a simple calculation suffices to show that it is not unreasonable as far as known geomagnetic field behaviour is concerned. The nine samples between depths of 27.52 and 27.76 m capture a systematic in-

clination change from $+71^\circ$ to -47° . At a sedimentation rate of 14 cm kyr^{-1} this change spans ~ 1400 yrs. Assuming the maximum possible declination change (180°) and an undiminished field strength of $60 \mu\text{T}$ (whereas SINT-800 suggests a global reduction of about 50 per cent), the annual change required is only 84 nT. Values exceeding this are found in the present-day secular variation, so there is no obvious reason to query the reality of this apparently

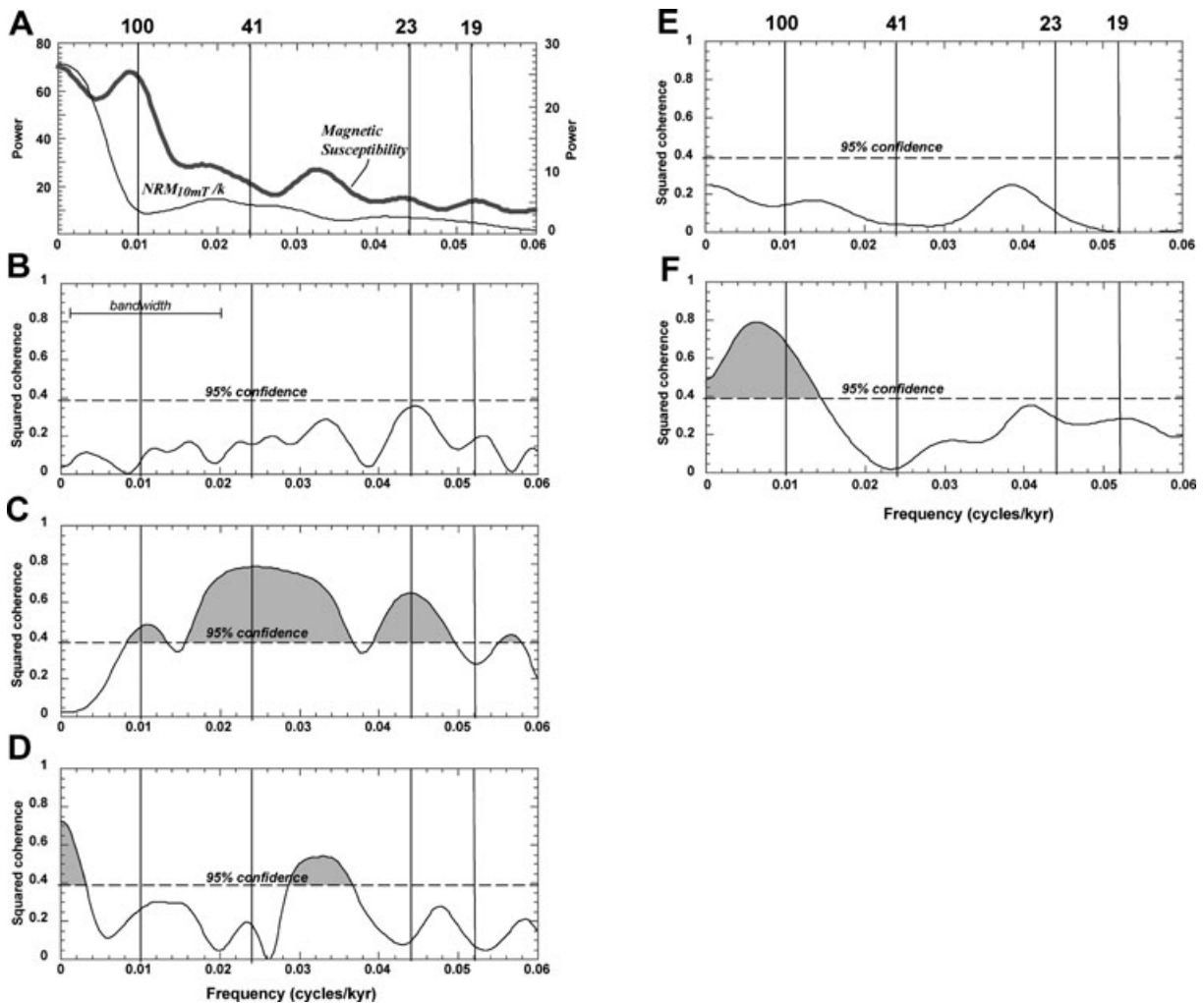


Figure 11. Power spectra (Blackman-Tukey method with a Bartlett window) of single sample magnetic susceptibility (thick line, right ordinate axis) and $\text{NRM}_{10\text{mT}/k}$ for BDP-93 entire hole 2 (A). The coherence between these two parameters with 95 per cent confidence level (horizontal dashed line) for the entire data set (B), for upper 15 m interval only (C), for the entire data set without the upper 15 m (D). The coherence between $\text{NRM}_{10\text{mT}/k}$ and ARM of hole 1 with 95 per cent confidence level for the entire data set (E) and the for upper 15 m interval only (F).

sudden onset. Following the comprehensive summaries of Oda *et al.* (2002) and Oda (2005), we conclude that this excursion is what they refer to as the Iceland Basin excursion which occurs near the base of oxygen isotope stage 6 (180–190 ka). They argue that it is distinct from the Jamaica/Pringle Falls excursion which occurred some 25 kyr earlier, and make the further important point that it corresponds to the minimum in SINT-800 at ~ 190 ka that Guyodo and Valet (1999) correlated, at that time, to the Jamaica/Pringle Falls excursion, but must now be considered to correspond to the Iceland Basin. We note that the actual shape of the excursion shown in Fig. 18 (two negative inclination troughs separated by a relative maximum) closely resembles that of the excursion reported by Oda *et al.* (2002).

One more event near 70 m was revealed in both holes (Fig. 19). This excursion has a complex shape in both holes and looks like a double event at least. The age of this feature corresponds to 480–495 ka that could be linked to the wide minimum between 480 and 500 ka in the SINT-800. This event could be the West Eifel excursion, originally dated by Schnepf and Hradetzky (1994) as 510 ± 30 . More recently Lund *et al.* (2001) have proposed an age of ~ 510 ka based their magnetic susceptibility correlation to SPECMAP in the

western North Atlantic. Uncertainly in the exact age of this excursion means that our identification is rather tentative.

CONCLUSIONS

The age model for both BDP-93 holes based on magnetic susceptibility, relative palaeointensity, biogenic silica data and U-Th absolute dating enables one to estimate a basal age of ~ 640 ka and an overall average deposition rate of $\sim 15 \text{ cm kyr}^{-1}$. Spectral analysis of the magnetic susceptibility and biogenic silica profiles indicate that Milankovitch signals are present. The ~ 100 kyr eccentricity, ~ 41 kyr obliquity and ~ 23 and ~ 19 kyr precession signals are all seen. A potentially important observation is the appearance of significant power at a ‘non-Milankovitch’ period of ~ 29 kyr, but it seems probable that this represents a sideband generated by frequency modulation.

The cores lie entirely in the Brunhes Chron as indicated by the stable remanence vectors of 1737 samples being almost all of normal polarity. The few intervals of low and/or negative inclinations probably represent real geomagnetic excursions, but only four of them can be identified with confidence. The first one is correlated to the

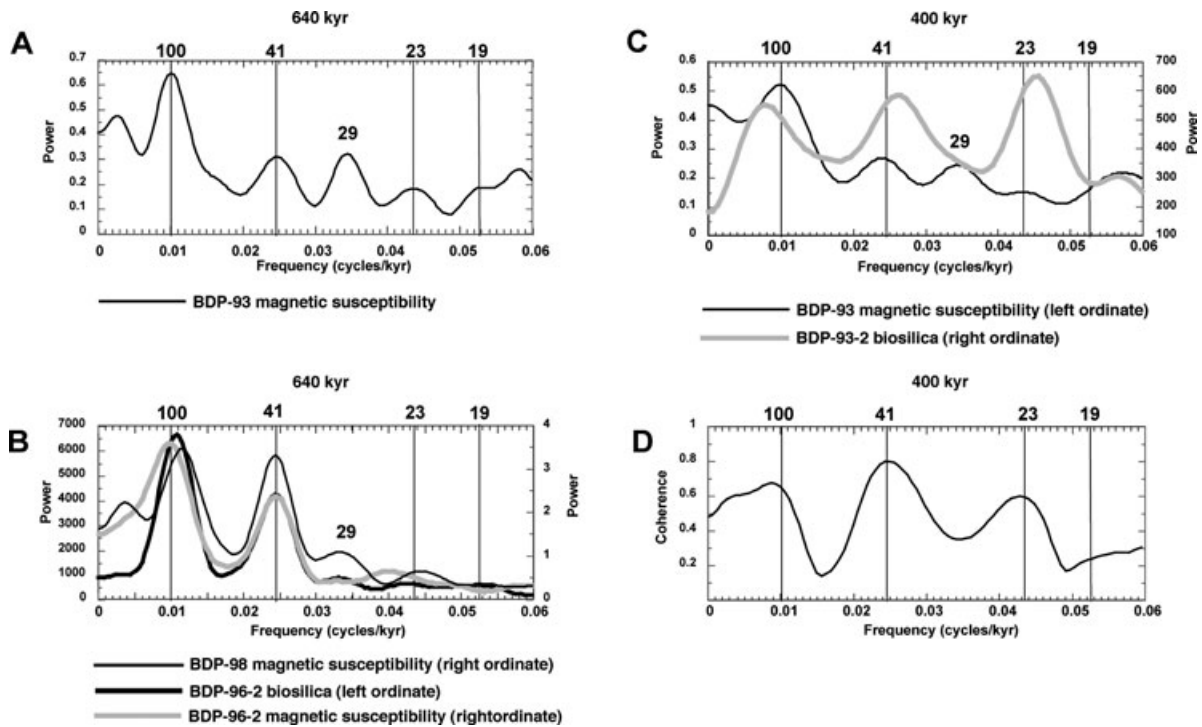


Figure 12. Frequency analysis of (A) the 640 kyr BDP-93 stacked magnetic susceptibility record (the analysis was performed using a 1-kyr step), (B) the 640 kyr BDP-98 magnetic susceptibility and the BDP-96-2 biogenic silica and magnetic susceptibility records [for (A) and (B), the analysis was performed using a 1-kyr step, signal bandwidth of 0.0078 and 192 lags], (C) the 400 kyr BDP-93 magnetic susceptibility and biogenic silica records (the analysis was performed using a 2-kyr step, signal bandwidth of 0.0125 and 60 lags) and (D) coherence of the two curves in (C). The confidence interval at the 90 per cent level is given by relation $0.54 < \Delta P/P < 2.53$ for all graphs. Vertical lines indicate the orbital (Milankovitch) periodicities (in kyr).

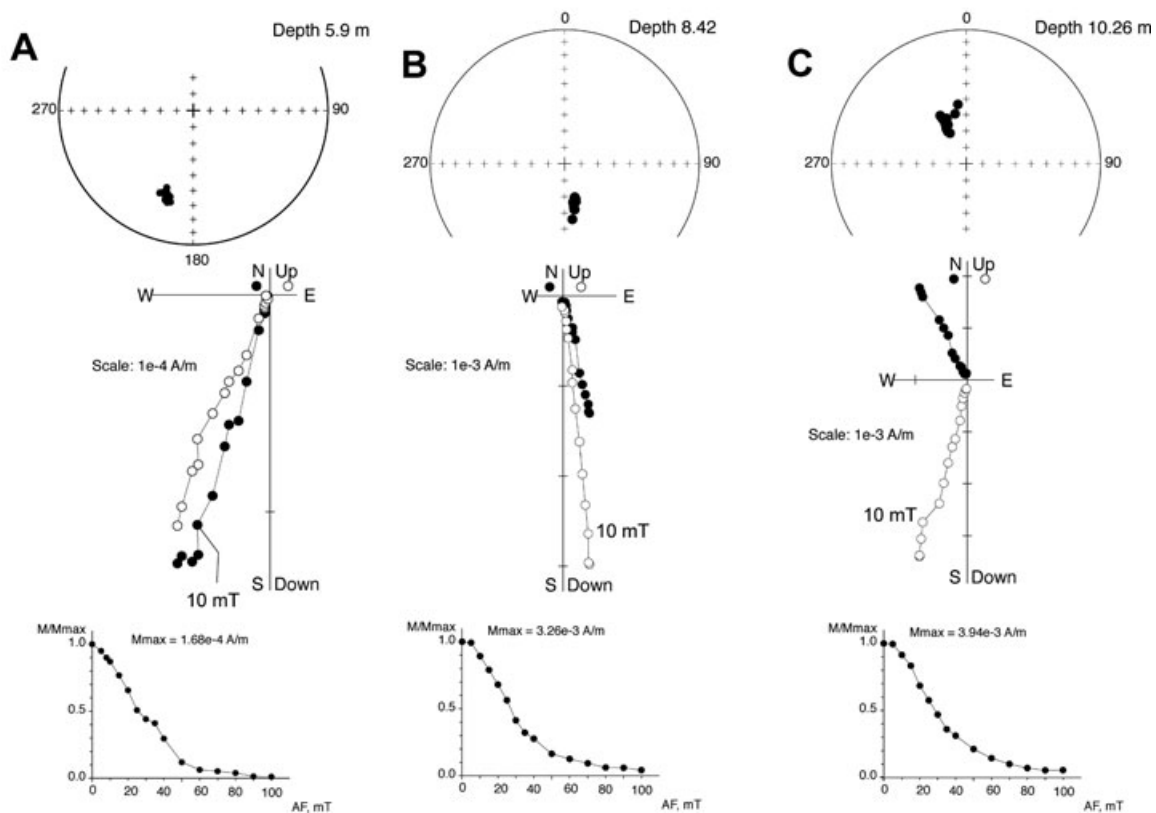


Figure 13. Examples of demagnetization behaviour of pilot samples from BDP-93-2. Closed (open) symbols in equal-area projections represent downward (upward) inclinations; closed (open) symbols in orthogonal plots represent projections onto the horizontal (vertical) plane. The core was not oriented azimuthally, so zero declination is arbitrary.

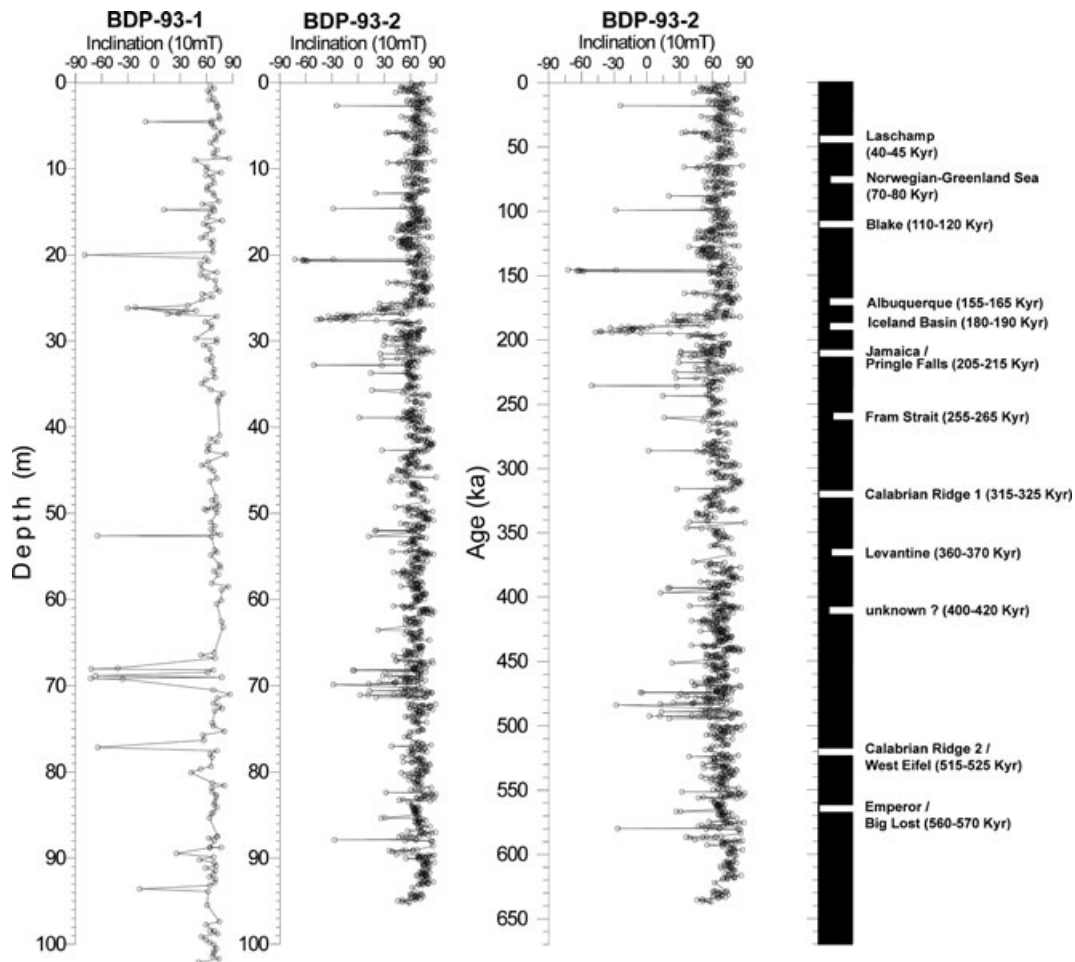


Figure 14. Inclination profiles for holes BDP-93-1 and BDP-93-2 versus depth and for BDP-93-2 versus time. The summary by Langereis *et al.* (1997) is given on the right, with additions.

Laschamp excursion (~ 38 ka), which is well known in many parts of the world. The second one is likely the Albuquerque excursion (~ 146 ka). There is still considerable uncertainty for the timing of this geomagnetic event. We suggest that the third one is the Iceland Basin excursion which occurred 180–190 ka ago, some 25 kyr later than the better-established Jamaica/Pringle Falls excursion. This interpretation requires that the intensity low in the SINT-800 summary that Guyodo and Valet (1999) correlate to the Jamaica/Pringle Falls excursion be re-assigned to the Iceland Basin excursion. The oldest event in our cores is tentatively identified as the West Eifel excursion (~ 480 – 495 ka) but again there currently exists significant uncertainty about the age of this geomagnetic event.

ACKNOWLEDGMENTS

We acknowledge Dr. M.A. Grachev from the Russian team, Dr. D. Williams from the U.S. team and Dr. H. Kawai from the Japanese team for considerable support of the Baikal Drilling Project. We thank V.F. Geletij, A.V. Goregljad, A.N. Gvozdkov, O.M. Khlystov, M.Z. Khuzin, K.M. Konstantinov, L.P. Koukhar, N.A. Sadovnikova and A.S. Zasiipkin for their help during the execution of this project and for participation in sampling and/or measuring. We are grateful to D.L. Paillard for providing his computer program Analyseries and J.-P. Cogné for providing his palaeomagnetic software PaleoMac (Cogné 2003). We also thank H. Oda, C. Langereis and an

anonymous reviewer for their thoughtful comments on this article. We are especially indebted to the entire BDP drilling team for providing such high quality cores, and to the Natural Sciences and Engineering Research Council of Canada for financial support to VAK and MEE. Part of the scientific and drilling work was supported by the Russian Academy of Sciences, NSF (grant EAR9317204) and Japanese fund.

REFERENCES

- Bassinot, F.C., Labeyrie, L.D., Vincent, E., Quidelleur, X., Shackelton, N.J. & Lancelot, Y., 1994. The astronomical theory of climate and the age of the Brunhes-Matuyama magnetic reversal, *Earth planet. Sci. Lett.*, **126**, 91–108.
- BDP-93 members, 1995. Results of the first drilled borehole at Lake Baikal near the Buguldeika Isthmus, *Russ. Geol. Geophys. J.*, **36**, 3–32. In Russian.
- BDP-93 members, 1997. Preliminary results of the first scientific drilling on lake Baikal, Buguldeika Site South-eastern Siberia, *Quat. Int.*, **37**, 3–17.
- Blackman, R.B. & Tukey, J.W., 1958. *The Measurement of Power Spectra from the Point of View of Communication Engineering*, Dover, New York.
- Blomendal, J., King, J.W., Hunt, A., DeMenocal, P.B. & Hayashida, A., 1993. Origin of the sedimentary magnetic record at Ocean Drilling Program sites on the Owen Ridge, Western Arabian Sea, *J. Geophys. Res.*, **98**, 4199–4219.

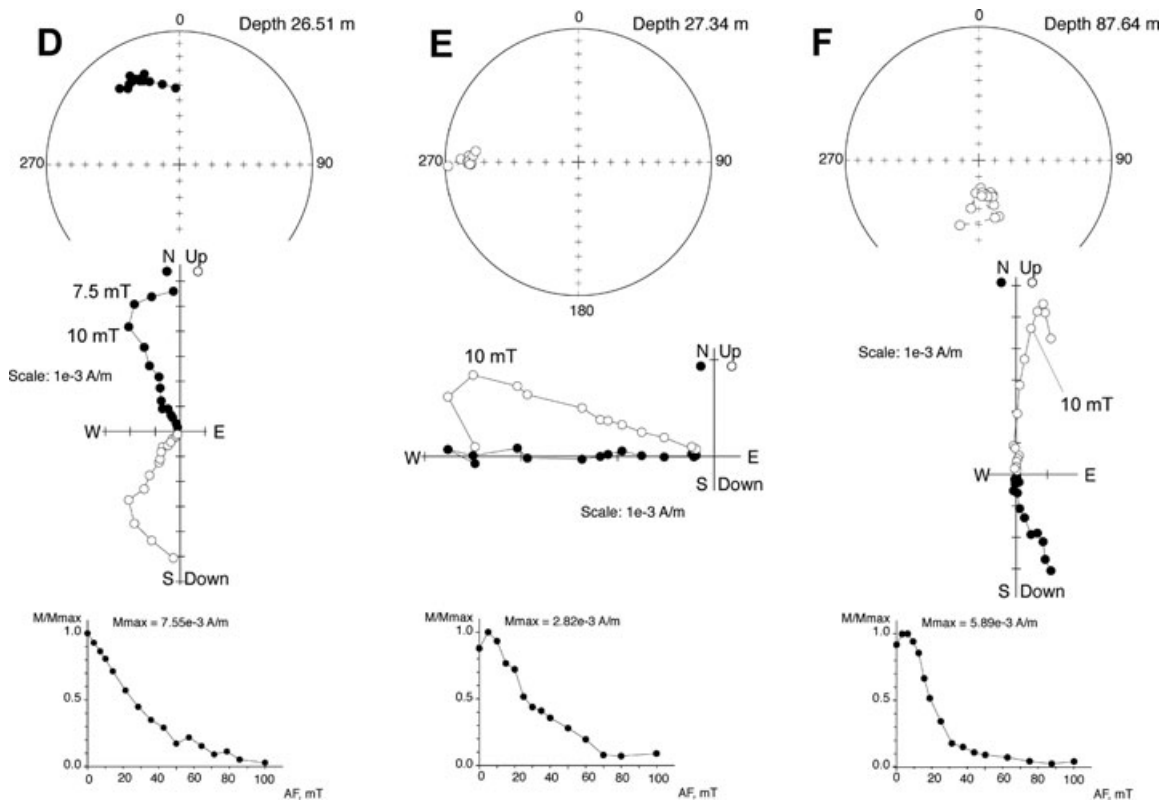


Figure 15. Examples of demagnetization behaviour of samples from possible geomagnetic excursions in core BDP-93-2. See Fig. 13 for definitions.

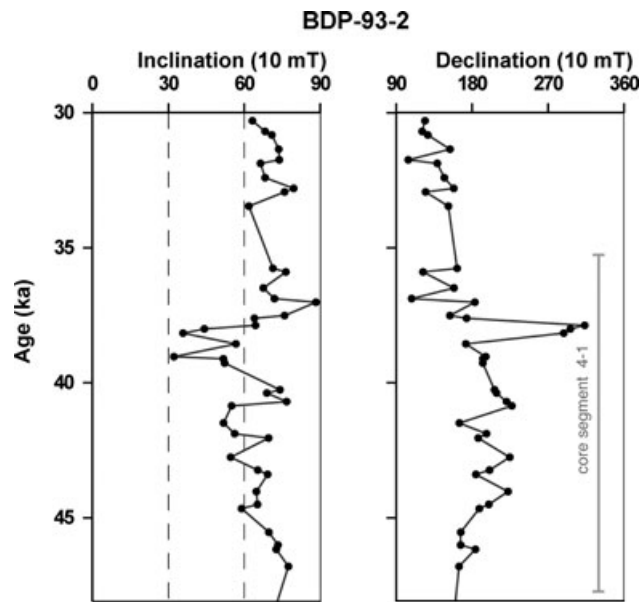


Figure 16. Inclination and relative declination patterns from core BDP-93-2 correlated to the Laschamp geomagnetic excursion. All inclinations and declinations are after 10 mT AF demagnetization. The extent of the core segment 4-1 is indicated.

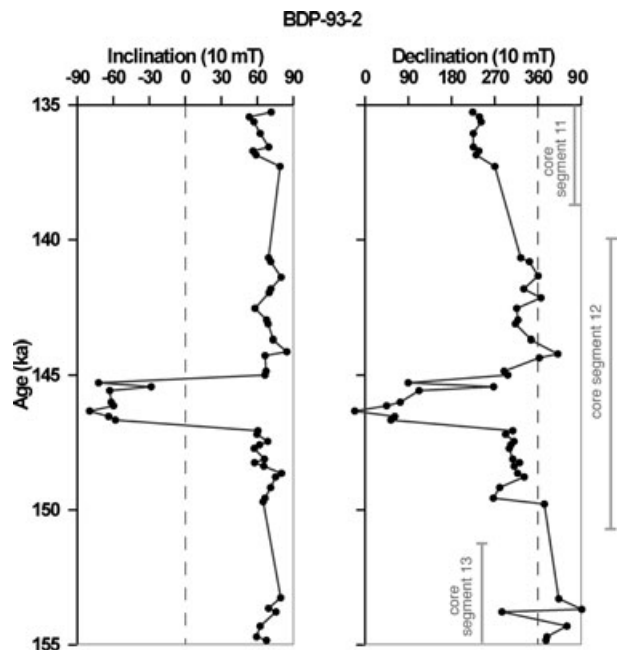


Figure 17. Inclination and relative declination patterns from core BDP-93-2 correlated to the Albuquerque geomagnetic excursion. All inclinations and declinations are after 10 mT AF demagnetization. The extent of the core segments 11, 12 and 13 are indicated.

Cogné, J.-P., 2003. PaleoMac: a Macintosh™ application for treating paleomagnetic data and making plate reconstructions, *Geochem. Geophys. Geosyst.*, 4(1), 1007, doi:10.1029/2001GC000227.

Colman, S.M., Peck, J.A., Hatton, J., Karabanov, E. & King, J., 1999. Biogenic silica records from the BDP93 drill site and adjacent areas of the Selenga Delta, Lake Baikal, *Siberia, J. Paleolimnol.*, 21, 9–17.

Guyodo, Y. & Valet, J.-P., 1999. Global changes in intensity of the Earth's magnetic field during past 800 kyr, *Nature*, 399, 249–252.

Dearing, J.A., Boyle, J.F., Appleby, P.G., Mackay, A.W. & Flower, R.J., 1998. Magnetic properties of recent sediments in Lake Baikal, Siberia, *J. Paleolimnol.*, 20, 163–173.

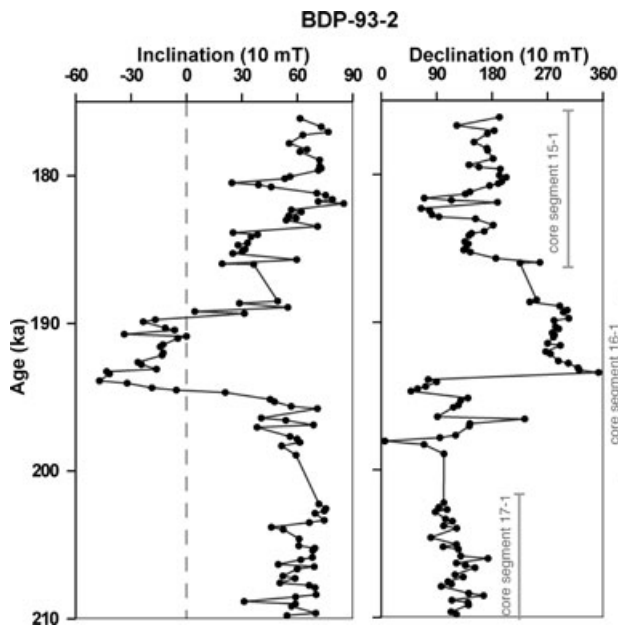


Figure 18. Inclination and relative declination patterns from core BDP-93-2 correlated to the Iceland Basin geomagnetic excursion. All inclinations and declinations are after 10 mT AF demagnetization. Core segments 15-1, 16-1 and 17-1 are indicated.

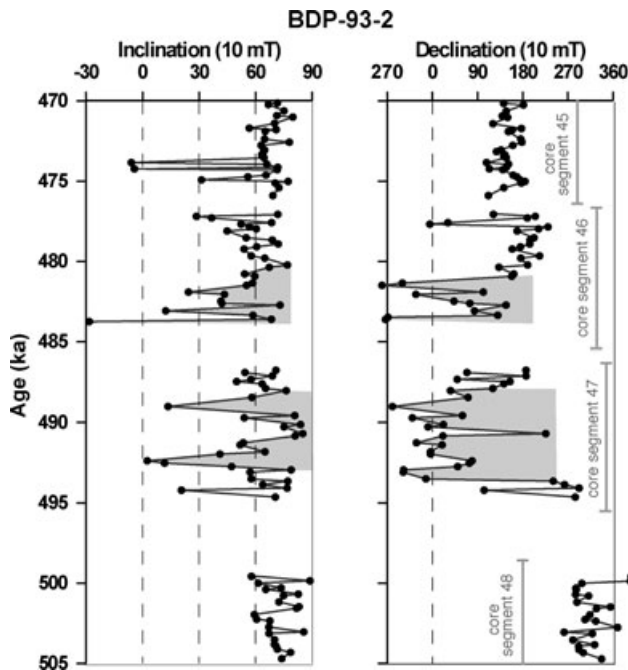


Figure 19. Inclination and relative declination patterns from core BDP-93-2 correlated to the West Eifel geomagnetic excursion. All inclinations and declinations are after 10 mT AF demagnetization. Core segments from 45 to 48 are indicated. Shaded areas indicate the excursion.

Demory, F., Nowaczyk, N.R., Witt, A. & Oberhänsli, H., 2005. High-resolution magnetostratigraphy of late quaternary sediments from Lake Baikal, Siberia: timing of intracontinental paleoclimatic responses, *Global Planet. Change*, **46**, 167–186.

Heller, F. & Evans, M.E., 1995. Loess magnetism, *Rev. Geophys. Space Phys.*, **33**, 211–240.

Hinnov, L.A., 2000. New perspectives on orbitally forced stratigraphy, *Annu. Rev. Earth Planet. Sci.*, **28**, 419–475.

Horii, M., Sakai, H., Kashiwaya, K., Nakamura, T. & Kawai, T., 2001. Rock-magnetic and granulometric studies of the BDP-93 cores, based on age model with ^{14}C dates and extrapolation, *Russ. J. Geol. Geophys.*, **42**, 175–185. In Russian.

Imbrie, J. *et al.*, 1984. The orbital theory of Pleistocene climate: Support from a revised chronology of the marine ISO record, in *Milankovitch and Climate, Part 1*, pp. 269–305, eds. Berger, A.L., Imbrie, J., Hays, J., Kukla, G. & Saltzman, B., Reidel, Hingham.

King, J.W., Banerjee, S.K. & Marvin, J., 1983. A new rock-magnetic approach to selecting sediments for geomagnetic paleointensity studies: application to paleointensity for the last 4000 yrs, *J. Geophys. Res.*, **88**(B7), 5911–5921.

King, J.W., Peck, J.A., Gangemi, P. & Kravchinskiy, V.A., 1993. Paleomagnetic and rock-magnetic studies of Lake Baikal, *Russ. Geol. Geophys.*, **34**(10–11), 174–192. In Russian.

Kravchinsky, A.Ya. & Mats, V.D., 1982. Paleomagnetism, in *Pliocene and Pleistocene of Central Baikal*, pp. 129–152, ed. Florensov, N.A., U.S.S.R., Nauka, Novosibirsk, In Russian.

Kravchinsky, V.A. *et al.*, 1998. Magnetostratigraphic scale of Central Asia Late Cenozoic under the data of deep drilling on Baikal, in *Global Changes of Natural Environment*, pp. 58–72, eds Dobretsov, N.L., Kovalenko, V.I., Global Changes of Natural Environment. Publishing House of Siberian Branch of Russian Academy of Sciences, Novosibirsk, in Russian.

Kravchinsky, V.A. *et al.*, 2003. Magnetic record of Lake Baikal sediments: chronological and paleoclimatic implication for the last 6.7 Myr. *Palaeogeogr., Palaeoclimatol., Palaeoecol.*, **195**, 281–298.

Langeris, C.G., Dekkers, M.J., de Lange, G.J., Paterne, M. & Santvoort, P.J.M., 1997. Magnetostratigraphy and astronomical calibration of the last 1.1 Myr from eastern Mediterranean piston core and dating of short events in the Brunhes, *Geophys. J. Int.*, **129**, 75–94.

Laskar, J., 1990. The chaotic motion of the solar system: a numerical estimate of the size of the chaotic zones, *Icarus*, **88**, 266–91.

Lund, S.P., Williams, T., Acton, G.D., Clement, B. & Okada, M., 2001. Brunhes Chron magnetic field excursions recovered from Leg 172 sediments, in *Proc. ODP Sci. Results*, Chapter 10, Vol. 172, pp. 1–18, eds Keigwin, L.D., Rio, D., Acton, G.D. & Arnold, E., Oceanic Drilling Program, College Station.

Maher, B.A., 1988. Magnetic properties of some synthetic sub-micron magnetites, *Geophys. J.*, **94**, 83–96.

Mats, V.D., 1993. The structure and development of the Baikal rift depression, *Earth Sci. Rev.*, **34**, 81–118.

Mix, A.C., Le, J. & Shackleton, N.J., 1995. Benthic foraminiferal stable isotope stratigraphy of site 846:0–1.8 Ma, in *Proc. ODP Sci. Results* Vol. **138**, pp. 839–847, ed. Pisias, Oceanic Drilling Program, College Station.

Oda, H., 2005. Recurrent geomagnetic excursions: a review for the Brunhes Normal Polarity Chron, *J. Geography (Chigaku Zasshi)*, **114**, 174–193 (in Japanese with English abstract).

Oda, H., Nakamura, K., Ikehara, K., Nakano, T., Nishimura, M. & Khlystov, O., 2002. Paleomagnetic record from Academician Ridge, Lake Baikal: a reversal excursion at the base of marine oxygen isotope stage 6, *Earth Planet. Sci. Lett.*, **202**, 117–132.

Opdyke, N.D. & Channell, J.E.T., 1996. *Magnetic Stratigraphy*, Academic Press, San Diego.

Paillard, D., Labeyrie, L. & Yiou, P., 1996. Macintosh program performs time-series analysis, *Eos Trans. AGU*, **77**, 379.

Peck, J.A. & King, J.W., 1996. Magnetofossils in the sediment of Lake Baikal, Siberia, *Earth Planet. Sci. Lett.*, **140**, 159–172.

Peck, J.A., King, J.W., Colman, S.M. & Kravchinsky, V.A., 1994. A rock-magnetic record from Lake Baikal, Siberia: evidence for Late Quaternary climate change, *Earth Planet. Sci. Lett.*, **122**, 221–238.

Peck, J.A., King, J.W., Colman, S.M. & Kravchinsky, V.A., 1996. An 84 Kyr Palaeomagnetic record from the sediments of Lake Baikal, Siberia, *J. Geophys. Res.*, **101**(B5), 11 356–11 385.

Plenier, G., Valet, J.-P., Guerin, G., Lefevre, J. & Carter-Stritz, B., 2006. Constraints on the age and Origin of the Laschamp Event in the Chaîne des Puys (France), *EOS Trans. AGU*, **87**(52), Fall Meet. Suppl., Abstract GP21B-1307.

- Rial, J., 1999. Pacemaking the ice ages by frequency modulation of Earth's orbital eccentricity, *Science*, **285**, 564–68.
- Rial, J., Anaclecio, C.A., 2000. Understanding nonlinear responses of the climate system to orbital forcing, *Quat. Sci. Rev.*, **19**, 1709–1722.
- Prokopenko, A.A. et al., 2001. Bogenic silica record of the Lake Baikal response to climatic forcing during the Brunhes, *Quat. Res.*, **55**, 123–132.
- Sakai, H. et al., 2001. Magnetic susceptibility studies on surface sediments of Lake Baikal and Lake Biwa, *Russ. Geol. Geophys. J.*, **42**(1–2), 56–63. In Russian.
- Sandimirov, I.V. & Pampura, V.D., 1995. The first experience of isochron dating of Baikal bottom sediments in core 295-k-2 and BDP93/1 by the method of uranium and thorium disequilibrium, *International Project on Paleolimnology and Late Cenozoic Climate Newsletter*, **9**, 31–34.
- Shackleton, N.J., Berger, A. & Peltier, W.R., 1990. An alternative astronomical calibration of the lower Pleistocene timescale based on ODP Site 677, *Trans. Roy. Soc. Edinburgh: Earth Sci.*, **81**, 251–261.
- Schnepp, E. & Hradetzky, H., 1994. Combined paleointensity and $^{40}\text{Ar}/^{39}\text{Ar}$ age spectrum data from volcanic rocks of the West Eifel field, Germany: evidence for an early Brunhes geomagnetic excursion, *J. Geophys. Res.*, **99**, 9061–9076.
- Takai, A., Shibuya, H. & Yoshihara, A. & Hamano, Y., 2002. Paleointensity measurements of pyroclastic flow deposits co-born with widespread tephra in Kyushu Island, Japan, *Phys. Earth Planet. Inter.*, **133**, 159–179.
- Tapponnier, P., Peltzer, G., Le Dain, A.Y., Armiji, R. & Cobbold, P., 1982. Propagating extrusion tectonics in Asia: New Insights from simple experiments with plasticine, *Geology*, **10**, 611–616.
- Tauxe, L., 1993. Sedimentary records of relative paleointensity of the geomagnetic field: theory and practice, *Rev. Geophys.*, **31**(3), 319–354.
- Thompson, R. & Oldfield, F., 1986. *Environmental Magnetism*, Allen & Unwin, London.
- Valet, J.P. & Meynadier, L., 1998. A comparison of different techniques for relative paleointensity, *Geophys. Res. Lett.*, **25**(1), 89–92.
- von Dobeneck, T. & Schmieder, F., 1999. Using rock magnetic proxy records for orbital tuning and extended times series analyses into the super- and sub-Milankovitch bands. in *Uses of Proxies in Paleoclimatology, Examples from the South Atlantic*, eds Fischer, G., Wefer, G., Springer, Berlin.
- Westgate, J.A., Stemper, B.A. & Pewe, T.L., 1990. A 3-My record of Pliocene-Pleistocene loess in interior Alaska, *Geology*, **18**(9), 858–861.
- Williams, D.F., Peck, J.A., Karabanov, E.B., Prokopenko, A.A. & Kravchinsky, V.A., 1997. Lake Baikal. Record of continental climate response to orbital insolation during the past 5 million yrs, *Science*, **278**, 1114–1117.
- Yu, L. & Oldfield, F., 1989. A multivariate mixing model for identifying sediment source from magnetic measurements, *Quat. Res.*, **32**, 168–181.